

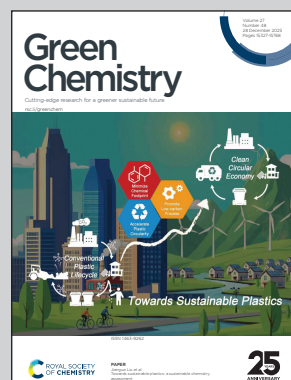
Showcasing research from Professor Deepti Kalsi's D-Kore lab - [K(C)atalysis for organics, Recycling & Environment], Department of Chemistry, IIT Bombay, Powai, Mumbai, India.

Metal free visible light mediated cycloaddition reaction using recyclable graphitic nitride under water

A sustainable, metal-free strategy for [2 + 2] photocycloadditions is presented using visible light and heterogeneous graphitic carbon nitride (g-CN). This method enables efficient cyclobutane formation from chalcone and styrene derivatives under mild conditions, avoiding noble metals and organic dyes. Mechanistic and DFT studies support an energy-transfer pathway, highlighting g-CN's capability beyond redox chemistry. This work showcases a green, scalable route to valuable cyclobutane frameworks.

Image reproduced by permission of Deepti Kalsi from *Green Chem.*, 2025, **27**, 15502.

## As featured in:



See Deepti Kalsi *et al.*, *Green Chem.*, 2025, **27**, 15502.



Cite this: *Green Chem.*, 2025, **27**, 15502

## Metal free visible light mediated cycloaddition reaction using recyclable graphitic nitride under water

Basavarajagouda E. Patil, Rahul Tarkase, Rajdeep Paul, Gopalan Rajaraman and Deepi Kalsi \*

The development of environmentally benign photocatalytic methodologies for [2 + 2] cycloadditions is of significant interest, given their utility in accessing cyclobutane motifs found in natural products and pharmaceuticals. Conventional approaches often rely on noble metal photocatalysts, harsh conditions, or organic dyes, limiting sustainability and scalability. Herein, we report a visible-light-driven, metal-free [2 + 2] photocycloaddition of chalcone and styrene derivatives using heterogeneous graphitic carbon nitride (g-CN). Mechanistic and DFT studies reveal an energy transfer (EnT) pathway rather than redox activation. This strategy demonstrates the potential of g-CN to expand beyond redox transformations toward sustainable energy-transfer-driven photocatalysis, offering a green and versatile route to cyclobutane frameworks.

Received 2nd September 2025,  
Accepted 7th November 2025

DOI: 10.1039/d5gc04611d  
[rsc.li/greenchem](http://rsc.li/greenchem)

### Green foundation

1. This work employs a metal-free, heterogeneous photocatalyst graphitic carbon nitride (g-CN) under visible-light irradiation, eliminating the need for precious or toxic metals and enabling catalyst recyclability for multiple cycles without significant loss of activity.
2. The [2 + 2] cycloaddition reactions were conducted in water as a reaction medium, avoiding hazardous organic solvents and aligning with the principles of safer solvents and auxiliaries. The protocol operates at ambient temperature and pressure, utilizing energy-efficient 427 nm visible-light sources. The direct cycloaddition strategy proceeds without the use of stoichiometric reagents, additives, or protecting groups, thereby minimizing waste generation and maximizing atom economy.
3. The methodology exhibited consistent reactivity and maintained product yields on the gram scale, underscoring its operational simplicity, practical scalability, and suitability for broader industrial applications. Furthermore, its integration with continuous-flow reactors holds significant promise for reducing reaction times and enhancing energy efficiency.

## Introduction

The development of sustainable, robust, and recyclable photochemical methodologies for the synthesis of valuable chemical entities has garnered significant attention in recent years. In light of growing global energy demands and environmental concerns, there is a need for green and energy-efficient synthetic strategies. Among various photochemical transformations<sup>1</sup> light-induced [2 + 2] cycloaddition of olefins has proven to be a powerful and atom-economical route for the construction of cyclobutane frameworks,<sup>2</sup> which are prevalent in numerous natural products and pharmaceuticals. Historically, photochemical processes have been dominated by noble metal-based photocatalysts, such as iridium, rhodium<sup>3</sup>

and organic dyes (Fig. 1a).<sup>4</sup> While these systems are often effective, they are limited by factors including high cost, limited availability, and the need for complex synthetic procedures. Moreover, traditional [2 + 2] cycloaddition reactions often face challenges such as extended reaction times, limited scalability, poor functional group tolerance, and reversibility. In addition, olefin isomerization frequently occurs under these conditions, leading to mixtures of stereo-isomeric products.<sup>5</sup> In this direction, various advancements have been made in recent years such as transitioning from UV<sup>6</sup> to visible light activation, adopting solid-state<sup>7</sup> over solution-phase systems, and designing both inter- and intramolecular reaction platforms to improve reactivities of cycloaddition reactions. In parallel, strategies have been explored to control regio- and stereoselectivity, such as the use of supramolecular hosts, templates, cage-like assemblies, and functionalized catalytic surfaces<sup>8</sup> to facilitate the coordination in the desired manner. Yet, only a few photocatalytic systems successfully merge sustain-

Department of Chemistry, IIT Bombay, Powai, Mumbai, 400076, India.  
 E-mail: [kdeepi@iitb.ac.in](mailto:kdeepi@iitb.ac.in)

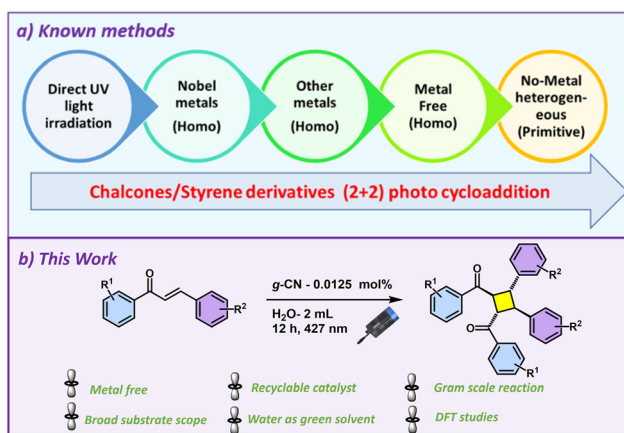


**Fig. 1** Synthesis of cyclobutane derivatives from chalcones and styrenes.

ability, reusability, simplicity, and broad applicability. An ideal photocatalyst would be electronically unbiased, accommodating both oxidative and reductive photo-redox pathways without substrate-specific limitations. Despite the widespread applicability of [2 + 2] cycloaddition strategies across different olefins, the development of a single catalyst system that can efficiently promote these reactions with diverse substrates such as chalcones and styrenes remains rare. In this context, graphitic carbon nitride (g-CN) emerges as a promising candidate. As a metal-free photocatalyst, it features a tuneable band gap, remarkable photostability, and facile synthesis. Its sustainable, reusable nature, coupled with adaptable electronic properties, makes g-CN highly suitable for a wide array of photocatalytic applications.<sup>9</sup> It has been successfully employed in diverse transformations including oxidation,<sup>10</sup> C–C coupling reactions,<sup>11</sup> reduction reactions,<sup>12</sup> and heteroatom coupling<sup>13</sup> primarily *via* redox pathways involving photoexcited electrons and holes. However, triplet energy transfer mechanisms, especially in [2 + 2] cycloadditions, remain underexplored.<sup>14</sup>

Styrene derivatives present additional challenges in photocycloadditions due to competing reactions like polymerization,<sup>15</sup> formation of oxidation side products<sup>16</sup> and requirement of higher triplet energies. While noble metal catalysts<sup>17</sup> and quantum dots have been employed for such transformations, there are only a few examples utilizing non-noble metals<sup>18</sup> and organic molecular catalysts.<sup>19</sup> Heterogeneous approaches have also shown considerable promise in this area. For instance, Yang *et al.*<sup>20</sup> employed g-CN in a flow reactor setup, while Wang *et al.* investigated inorganic semiconductors such as  $\text{Ag}_3\text{PO}_4$  specifically for anethole derivatives.<sup>21</sup> Additionally, Hashimoto *et al.* utilized  $\text{TiO}_2$  under UV light to facilitate [2 + 2] cycloadditions of enol ether olefins.<sup>22</sup> Despite these efforts, substrate scope and energy efficiency remain limiting factors for the reported reactions. However, these catalytic systems showed an oxidative mechanism as these substrates have lower oxidation potential compared to the catalysts and easily undergo oxidation to generate the cationic radical while remaining unreactive for substrates with higher redox potentials.

In this study, we present a visible-light-mediated [2 + 2] photoredox cycloaddition strategy for chalcone and styrene derivatives, employing a heterogeneous and recyclable g-CN photocatalyst (Fig. 1b) undergoing a triplet energy transfer mechanism unlike that reported by Wang *et al.*<sup>21</sup> This likely arises from the photoactive substrates enabling localized triplet excitation.<sup>23</sup> In particular, chalcone derivatives enable efficient intersystem crossing from the singlet to the triplet state, thereby promoting the energy transfer pathway (EnT). As a result, cross-dimerization products were not observed, even in the presence of electrophilic olefins.

## Results and discussion

The synthesis and characterization of the catalysts were carried out to assess their structural and catalytic properties. g-CN was synthesized using different precursors (see SI section 2). Different batches of catalysts were prepared by varying precursors such as melamine (MCN), urea (UCN) and dicyandiamide (DCN) to investigate their influence on the material structure and functionality. All three samples exhibited comparable FTIR stretching vibrations, UV-visible absorption spectra, and optical band gaps as determined from Tauc plots (Fig. 2), which were consistent with previously reported values, indicating similar chemical functionalities and electronic structures. TGA analysis also indicated a high thermal stability for all three catalysts (Fig. 2d, e and f). Despite these similarities, differences emerged in surface area and crystallinity, as revealed by nitrogen sorption and powder X-ray diffraction (P-XRD) analyses (Fig. 2c). The sample derived from urea (UCN) exhibited a higher surface area compared to MCN and DCN. However, UCN showed less intense P-XRD peaks, suggesting a thinner layered structure compared to the other two. These observations were subsequently supported by scanning electron microscopy (SEM) (Fig. S1), which revealed a more exfoliated morphology in the case of the urea derived catalyst (UCN) compared to the thicker, aggregated layers seen in the other samples. In addition to the pristine materials, an oxidized variant of g-CN (OCN) and a physically modified sample bearing adsorbed *p*-toluenesulfonyl chloride (TCN) were synthesized and characterized. To evaluate their practical relevance, the catalytic activities of all materials were tested under identical reaction conditions, allowing a direct comparison of their structure–activity relationships.

The synthesized catalysts were subsequently evaluated for their activity in the [2 + 2] photocycloaddition of olefins. Initial trials using the model substrate (**1a**) in acetonitrile (entry 1, Table 1) successfully yielded the desired cyclobutane product. A systematic solvent screening examined the influence of solvents on photocatalytic efficiency. Polar aprotic solvents such as DMF (entry 2, Table 1) gave an 8% yield. Protic solvents exhibited mixed behaviour; methanol (entry 3, Table 1) provided a moderate yield of 33%. Moderately polar aprotic solvents such as THF, dichloromethane (DCM), and 1,4-dioxane (entries 4–6, Table 1) delivered improved yields ranging from

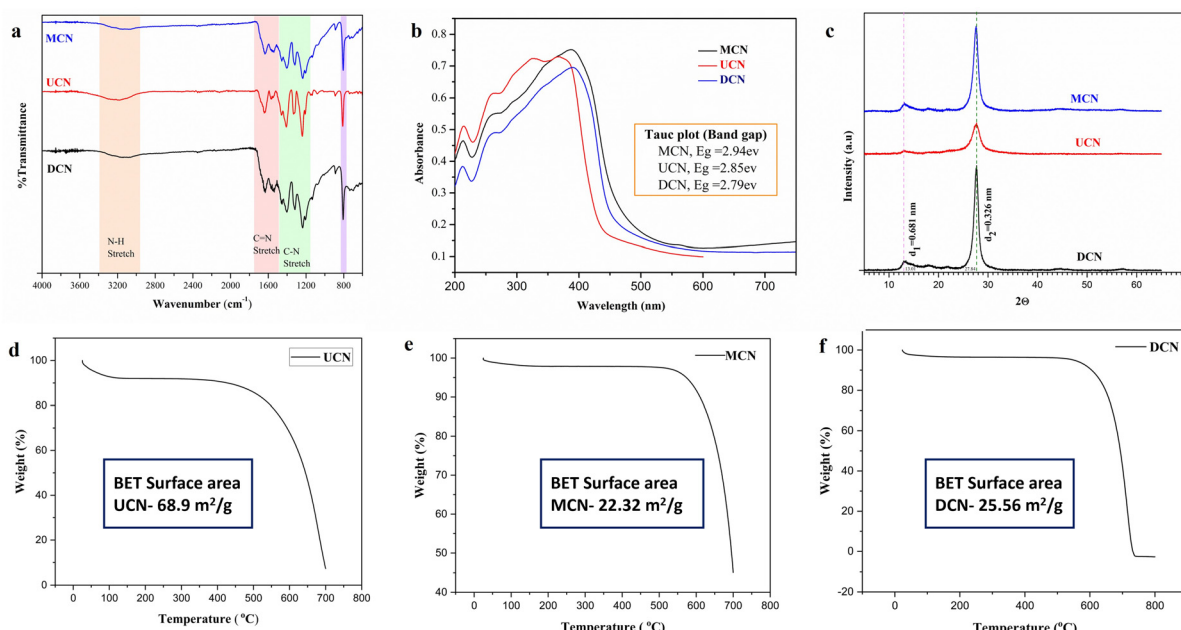
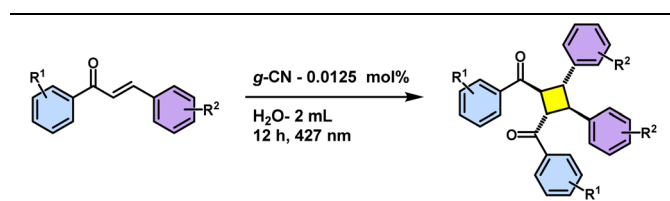


Fig. 2 (a) IR spectra of catalysts, (b) UV/Vis absorption spectra of catalysts, (c) P-XRD spectra of catalysts, (d) TGA of UCN, (e) TGA of MCN and (f) TGA of DCN.

40 to 66%. Nonpolar or weakly polar solvents showed the best performance, with pentane and benzene (entries 7 and 8, Table 1) affording the yields of 74% and 82%, respectively. In particular, benzene may enhance  $\pi$ - $\pi$  stacking interactions with the g-CN surface, while the non-coordinating nature of these solvents minimizes catalyst passivation. Nitromethane (entry 9, Table 1) gave a 55% yield. Water was tested as a green solvent and delivered yields of 39%, 70%, and 47% at different substrate concentrations (entries 10–12, Table 1). The best yield (70%, entry 11) was observed at 0.125 M, likely due to hydrophobic aggregation that brings reactants closer and improves charge transfer, as reported by Fu *et al.*<sup>24</sup> On the other hand, when 0.25 M water was used, there was a decline in yield (47%) (entry 12, Table 1) likely due to diffusion limitations or catalyst aggregation.<sup>25</sup> Catalyst screening at 0.125 M indicated that melamine-derived g-CN (MCN) was most effective, producing a 70% yield (entry 11, Table 1), likely due to favourable bandgap alignment and surface properties. In contrast, g-CN synthesized from urea (UCN) and dicyandiamide (DCN) led to lower yields of 64% and 49%, respectively (entries 13 and 14, Table 1) underscoring the importance of precursor selection in tailoring catalytic performance. Acid functionalized g-CN (OCN) and physically adsorbed *p*-tolyl sulphonyl chloride (TCN) on g-CN were also tried and they provided yields of 28% and 45%, respectively (entries 15 and 16, Table 1). A comparison with homogeneous organic photocatalysts further contextualized the aqueous-phase performance of g-CN. For example, Eosin Y (entry 17, Table 1) enabled a yield of 54%, while 4-CzPIN and thianthrene (entries 18 and 19, Table 1) furnished 56% and 58% yields, respectively, under the aqueous conditions. Although direct comparison is chal-

lenging due to catalyst differences, MCN showed higher yields under identical conditions. Control experiments showed that both light and a catalyst were essential for the reaction. No product formed in the dark (entry 22, Table 1), and only 10% yield was obtained without the catalyst (entry 23, Table 1), confirming the necessity of both light and the catalyst. Under an oxygen atmosphere, the reaction afforded 40% yield (entry 24, Table 1), suggesting triplet state quenching by oxygen. Doubling the catalyst loading reduced the yield to 32% (entry 25, Table 1). Extending the reaction time to 24 h offered no improvement over the 12 h result.

Furthermore, various chalcones were evaluated under the optimized conditions to understand the electronic and steric effects on the reaction. For example, *para*-methoxy-substituted chalcones **1a** and **1c** (Scheme 1) delivered the desired cycloadducts in 70% and 68% yields, respectively. In contrast, sterically hindered substrates like the *ortho*-methoxy derivative **1d** afforded a moderate yield of 50%. Exploration of electron-deficient substrates provided additional insights into the reaction scope. The *para*-nitro-substituted chalcone **1h** (Scheme 1) presented marked challenges because it was known to undergo rapid isomerization<sup>5</sup> and typically resist transformation under photochemical conditions. While the yield in this case was moderate, it nonetheless highlights the ability of g-CN to enable transformations of electron poor substrates as well. Building on these findings, the methodology was extended to  $\alpha,\beta$ -unsaturated carbonyl compounds, such as benzylidene acetone **1j** (Scheme 1), which furnished the corresponding product in 55% yield. This demonstrates the broader applicability of the protocol beyond chalcone derivatives. Hetero-aromatic substrates **1k**, **1l** and **1m** were also well-

**Table 1** Optimization for the photochemical [2 + 2] cycloaddition of chalcones

Entry	Catalyst	$\lambda$ (nm)	Solvent	Yield (%)
1	MCN	427	ACN	12
2	MCN	427	DMF	8
3	MCN	427	MeOH	33
4	MCN	427	THF	40
5	MCN	427	DCM	60
6	MCN	427	1,4-Dioxane	66
7	MCN	427	Pentane	74
8	MCN	427	Benzene	82
9	MCN	427	Nitromethane	55
10	MCN	427	H <sub>2</sub> O (0.080 M)	39
11	MCN	427	H <sub>2</sub> O (0.125 M)	70
12	MCN	427	H <sub>2</sub> O (0.25 M)	47
13	UCN	427	H <sub>2</sub> O	64
14	DCN	427	H <sub>2</sub> O	49
15	OCN	427	H <sub>2</sub> O	28
16	TCN	427	H <sub>2</sub> O	45
17	Eosin Y	427	H <sub>2</sub> O	54
18	4-CzPIN	427	H <sub>2</sub> O	56
19	Thianthrene	427	H <sub>2</sub> O	58
20	MCN	Blue LED	H <sub>2</sub> O	Trace
21	MCN	390	H <sub>2</sub> O	65
22	MCN	—	H <sub>2</sub> O	n.r.
23	—	427	H <sub>2</sub> O	10
24 <sup>a</sup>	MCN	427	H <sub>2</sub> O	40
25 <sup>b</sup>	MCN	427	H <sub>2</sub> O	32

Reaction conditions: **1** (0.25 mmol), MCN (1.25 mmol), H<sub>2</sub>O 2 mL (0.125 M), irradiation under 427 nm in N<sub>2</sub>, at room temperature for 12 h. <sup>a</sup>Reaction performed in the presence of an oxygen atmosphere.

<sup>b</sup>Reaction performed with 6 mol (40 mg) of catalyst.

tolerated under the reaction conditions (Scheme 1) to access structurally diverse products. However, styrene and stilbenes were found to be unreactive under the optimised conditions.

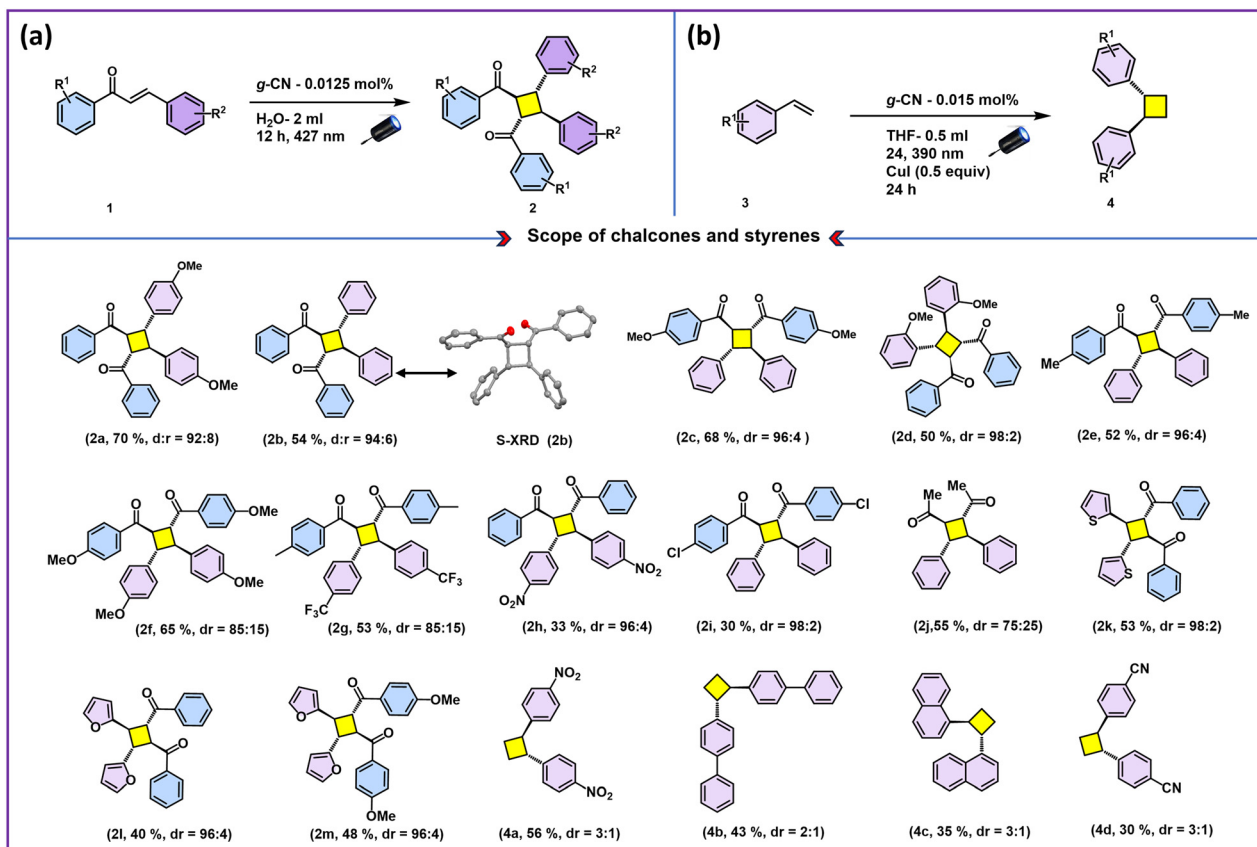
To gain a better understanding of the system and its reactivity pattern DFT calculations were performed (see SI section 9). The HOMO–LUMO gaps for chalcones were found to be 3.335 eV to 3.553 eV, which lie higher than the pristine g-CN band gap (2.49 eV). This suggests that chalcones can act as efficient light absorbers in the visible region and complement the photocatalytic activity of g-CN. The analysis of the molecular orbital composition shows that the HOMO is delocalized across the phenyl and enone backbone, with a significant contribution from O-2p lone pair orbitals, imparting a nucleophilic character. The LUMO, on the other hand, is a  $\pi$  orbital localized primarily on the carbonyl and conjugated C=C bond, marking these sites as the most probable locations for photochemical activation. This spatial distribution is crucial: the oxygen atom anchors the HOMO energetically, while the conjugated  $\pi^*$  system stabilizes the LUMO, thereby facilitating efficient  $\pi$ - $\pi^*$  transitions under irradiation. Substituent effects

play a defining role in tuning the electronic properties of chalcones. Electron-donating groups such as -OMe on the aromatic rings stabilize the HOMO by donating electron density into the conjugated backbone, thereby narrowing the HOMO–LUMO gap and enhancing light absorption in the visible range. This correlates well with experimental observations, where methoxy-substituted chalcones showed higher yields and faster reaction rates under g-CN photocatalysis. Conversely, electron-withdrawing substituents destabilize the LUMO and widen the HOMO–LUMO gap (>3.8 eV), shifting absorption to the UV region and reducing overlap with the g-CN conduction band. These chalcones indeed showed diminished reactivity in the experimental screening, consistent with the electronic structure rationale.

Photophysically, the relatively small HOMO–LUMO gap (~3.3 eV) and the conjugated  $\pi$ -system allow chalcones to undergo efficient intersystem crossing (ISC) from the singlet to the triplet manifold. This property is key for the [2 + 2] photocycloaddition mechanism, which relies on the participation of the triplet-excited state of the chalcone. DOS results (Fig. S9) confirm that the oxygen and conjugated carbons contribute significantly near the Fermi level, meaning that both the n  $\rightarrow$   $\pi^*$  and  $\pi$   $\rightarrow$   $\pi^*$  transitions are energetically accessible. This dual channel explains why chalcones serve as excellent triplet acceptors during energy transfer from excited g-CN. Taken together, the electronic structure analysis clarifies that chalcones are not passive reactants but active participants in the photocatalytic cycle. Their frontier orbital energies align well with the band edges of g-CN, enabling both (i) energy transfer from photoexcited g-CN to populate the chalcone triplet state and (ii) weak charge transfer interactions that slightly reduce the composite band gap (2.31 eV), thereby facilitating visible-light reactivity. This synergy between chalcone's intrinsic photophysics and g-CN's semiconducting properties underpins the observed selectivity and efficiency in the photocycloaddition reaction. All the HOMO and LUMO of some of the selected molecules have been plotted in Fig. 3 with a contour value of 0.03 along with their energy values in eV. The substrates such as unsubstituted styrene and stilbene (*cis* and *trans*) failed to show any reactivity under the optimized conditions. The fact was also evident from the HOMO–LUMO gap which was found to be higher than 3.8 eV (Fig. 3).

In addition, catalyst recyclability was tested over four cycles using model substrate **1a** (Scheme 1) and UCN proved the catalyst efficiency (Fig. S2). To evaluate the practical applicability of the method, a gram-scale reaction was conducted using 1 g of chalcone substrate under the optimized photocatalytic conditions. The reaction proceeded smoothly and produced 765 mg of the cyclobutane product (**2a**), corresponding to a 76% isolated yield. A detailed experimental procedure is available in the SI. Notably, the yield was slightly higher than that obtained under small-scale conditions, demonstrating both the efficiency of g-CN as a photocatalyst and the scalability of the methodology.

Encouraged by the success with chalcones, we next turned our attention to electronically distinct styrene derivatives,



**Scheme 1** Substrate scope of chalcone and styrene. Conditions: (a) 1 (0.25 mmol), MCN (1.25 mmol, MW = 637.262), H<sub>2</sub>O = 2 mL (0.125 M), irradiation under 427 nm in N<sub>2</sub>, at room temperature for 12 h. (b) 3 (1 mmol), MCN (1.5 mmol), CuI (0.5 mmol), and THF = 0.5 mL.

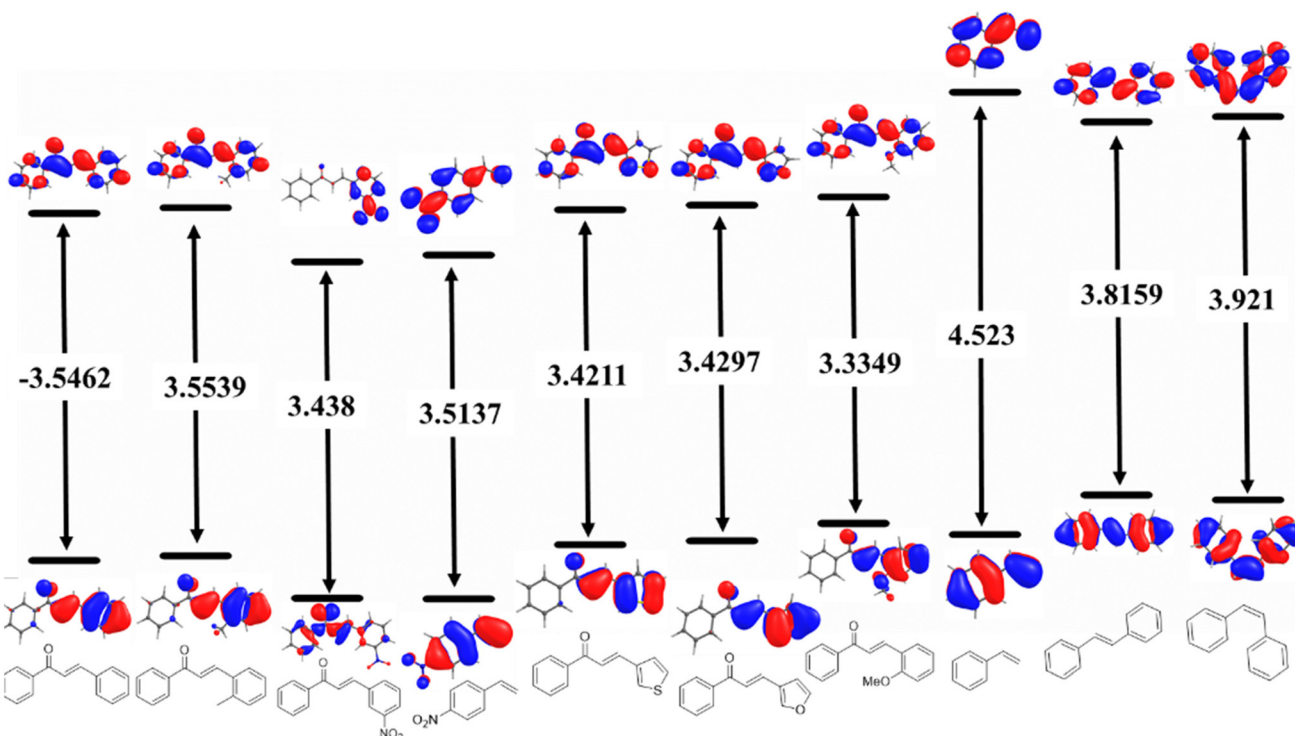


**Table 2** Controlled reactions

Additive	Chalcone (yield)	Styrene (yield)
KI	40	30
CuI	53	56
CuCl <sub>2</sub>	56	50
AgNO <sub>3</sub>	50	49
TEA	32	Trace
TEMPO	38	Trace

employing THF as the solvent and urea derived g-CN (UCN) as a photocatalyst. Initial attempts using unsubstituted styrene resulted in only trace product formation, indicating limited reactivity under standard reaction conditions. However, when *para*-nitro-substituted styrene **3a** (Scheme 1) was tested, notably 12% yield of the product was obtained after 24 h irradiation under a blue LED which was later optimised to 56% in 12 h using 390 nm irradiation. Complementing these findings, CuI (0.5 equiv.) was shown to positively affect the reaction. In addition to this, structurally diverse styrene derivatives such as 4-vinyl biphenyl **3b** (Scheme 1), 43%, and 1-vinyl naphthalene **3c** (Scheme 1), 35%, were also explored. Although these systems are not inherently electron-deficient, they undergo [2 + 2] cycloaddition under optimized conditions, indicating that a  $\pi$ -conjugated substrate can also be accommodated. Although the conversions are moderate, these transformations are rarely achieved using heterogeneous photocatalysts<sup>26</sup> and are generally reported *via* alternative, homogeneous photochemical methods instead. To probe the reaction mechanism, quenching experiments (Table 2) with radical scavengers such as TEMPO and electron donors like triethylamine were performed. A notable drop in reactivity was observed, which suggested that radical chain propagation is not a dominant mechanism in this case. Additionally, Cu(I) and Cu(II) salts were found to enhance product yields, possibly through Lewis acid coordination with the alkene or intermediates, thus facilitating triplet energy transfer or suppressing undesired pathways (Fig. S5 and S6). This result highlights the energy transfer capability of urea-derived graphitic carbon nitride (UCN). Notably, the performance emphasizes the untapped potential of g-CN in triplet-sensitized photochemical transformations.

## Conclusions

In summary, a sustainable and operationally simple metal-free [2 + 2] cycloaddition strategy using a heterogeneous graphitic carbon nitride (g-CN) photocatalyst under visible-light irradiation was developed. The protocol proceeds efficiently in water, a green solvent, without the use of precious metals, additives, or harsh conditions, aligning with the key principles of green chemistry. Mechanistic studies confirmed the non-radical nature of the process and the absence of cross-dimerization, showcasing the selectivity and robustness of the system. This was also supported by DFT calculations. The protocol was successfully scaled to gram quantities without com-

promising the efficiency of the protocol and offers a green and versatile alternative for constructing cyclobutane frameworks under ambient and eco-friendly conditions. These findings underscore the broader potential of g-CN to drive energy transfer mediated transformations, opening avenues for selective, metal-free synthesis of complex molecular scaffolds under environmentally benign conditions.

## Author contributions

D. K. and B. P. conceptualized, designed the project and wrote the manuscript. R. T. assisted in performing the substrate scope studies. G. R. and R. P. contributed to the DFT calculations.

## Conflicts of interest

There are no conflicts to declare.

## Data availability

The data supporting this article have been included as part of the supplementary information (SI). Supplementary information: procedure, NMR, HRMS, Uv-Vis, IR, single crystal XRD, P-XRD, BET, TGA and SEM analyses and DFT calculations. See DOI: <https://doi.org/10.1039/d5gc04611d>.

## Acknowledgements

Financial support provided by the Indian Institute of Technology Bombay through an initiation grant (Spons/CH/10002103-1/2024) and research funding from the Science and Engineering Research Board (SERB) (SRG/2023/001029) India is gratefully acknowledged. G. R. acknowledges SERB India for funding (CRG/2022/001697; SB/SJF/2019-20/12). B. P. and R. T. acknowledge the IITB for their fellowships and R. P. acknowledges the financial support from the Prime Minister's Research Fellowship (PMRF).

## References

- 1 B. König, *Eur. J. Org. Chem.*, 2017, 1979–1981.
- 2 (a) S. Poplata, A. Tröster, Y. Q. Zou and T. Bach, *Chem. Rev.*, 2016, **116**, 9748–9815; (b) J. Li, K. Gao, M. Bian and H. Ding, *Org. Chem. Front.*, 2019, **6**, 3625–3630; (c) Y. Cai, J. Zhao and Z. Wang, *Org. Chem. Front.*, 2020, **7**, 136–154; (d) S. Y. Hou, B. C. Yan, H. D. Sun, *et al.*, *Nat. Prod. Bioprospect.*, 2024, **14**, 37.
- 3 (a) K. Teegardin, J. I. Day, J. Chan and J. Weaver, *Org. Process Res. Dev.*, 2016, **20**, 1156–1163; (b) J. Twilton, C. C. Le, P. Zhang, M. H. Shaw, R. W. Evans and D. W. C. MacMillan, *Nat. Rev. Chem.*, 2017, **1**, 0052.

4 (a) F. Strieth-Kalthoff and F. Glorius, *Beilstein J. Org. Chem.*, 2020, **16**, 1163–1187; (b) A. Tlili and M. Lakhdar, *J. Org. Chem.*, 2016, **81**(16), 7157–7161; (c) A. Joshi-Pangu, F. Lévesque, H. G. Roth, S. F. Oliver, L.-C. Campeau, D. Nicewicz and D. A. DiRocco, *J. Org. Chem.*, 2016, **81**, 7244–7249.

5 (a) S. K. Pagire, A. Hossain, L. Traub, S. Kerres and O. Reiser, *Chem. Commun.*, 2017, **53**, 12064–12067; (b) J. B. Metternich and R. Gilmour, *J. Am. Chem. Soc.*, 2015, **137**, 11254–11257.

6 R. G. Salomon, *Tetrahedron*, 1983, **39**, 485–575.

7 (a) K. Biradha and R. Santra, *Chem. Soc. Rev.*, 2013, **42**, 950–967; (b) V. Ramamurthy and J. Sivaguru, *Chem. Rev.*, 2016, **116**, 9914–9993; (c) X. Song, J. Gu, E. Zhang, Y. Jiang, M. Xin, Y. Meng, A. S. C. Chan and Y. Zou, *ACS Sustainable Chem. Eng.*, 2022, **10**, 16399–16407.

8 (a) Y. Jiang, R. López-Arteaga and E. A. Weiss, *J. Am. Chem. Soc.*, 2022, **144**, 3782–3786; (b) Y.-L. Lu, Y.-H. Qin, S.-P. Zheng, J. Ruan, Y.-H. Huang, X.-D. Zhang, C.-H. Liu, P. Hu, H.-S. Xu and C.-Y. Su, *ACS Catal.*, 2024, **14**, 94–103; (c) J.-S. Wang, K. Wu, C. Yin, K. Li, Y. Huang, J. Ruan, X. Feng, P. Hu and C.-Y. Su, *Nat. Commun.*, 2020, **11**, 4675; (d) Y. Jiang, C. Wang, C. R. Rogers, M. S. Kodaimati and E. A. Weiss, *Nat. Chem.*, 2019, **11**, 1034–1040; (e) K. S. S. P. Rao, S. M. Hubig, J. N. Moorthy and J. K. Kochi, *J. Org. Chem.*, 1999, **64**, 8098–8104; (f) M.-M. Gan, J.-G. Yu, Y.-Y. Wang and Y.-F. Han, *CrystEngComm*, 2018, **18**, 553–565.

9 (a) Y. Wang, X. Wang and M. Antonietti, *Angew. Chem., Int. Ed.*, 2012, **51**, 68–89; (b) A. Savateev, I. Ghosh, B. König and M. Antonietti, *Angew. Chem., Int. Ed.*, 2018, **57**, 15936–15947; (c) K. S. Lakhi, D.-H. Park, K. Al-Bahily, W. Cha, B. Viswanathan, J.-H. Choy and A. Vinu, *Chem. Soc. Rev.*, 2017, **46**, 72–101; (d) X. Wang, K. Maeda, A. Thomas, K. Takanabe, G. Xin, J. M. Carlsson, K. Domen and M. Antonietti, *ACS Catal.*, 2012, **2**, 1596–1606; (e) M. Marchi, G. Gentile, C. Rosso, M. Melchionna, P. Fornasiero, G. Filippini and M. Prato, *ChemSusChem*, 2022, **15**, e2022010; (f) S. K. Verma, R. Verma, Y. R. Girish, F. Xue, L. Yan, S. Verma, M. Singh, Y. Vaishnav, A. B. Shaik, R. R. Bhandare, K. P. Rakesh, K. S. Sharath Kumar and K. S. Rangappa, *Green Chem.*, 2022, **24**, 438–479; (g) B. Dam, B. Das and B. K. Patel, *Green Chem.*, 2023, **25**, 3374.

10 (a) Y. Xiao, G. Tian, W. Li, Y. Xie, B. Jiang, C. Tian, D. Zhao and H. Fu, *J. Am. Chem. Soc.*, 2019, **141**, 2508–2515; (b) M. Marchi, G. Gentile, C. Rosso, M. Melchionna, P. Fornasiero, G. Filippini and M. Prato, *ChemSusChem*, 2022, **15**, e2022010; (c) Y. Wang, H. Li, J. Yao, X. Wang and M. Antonietti, *Chem. Sci.*, 2011, **2**, 446–450; (d) Y. Wang, J. Zhang, X. Wang, M. Antonietti and H. Li, *Angew. Chem., Int. Ed.*, 2010, **49**, 3356–3359; (e) X. Xiao, Y. Gao, L. Zhang, J. Zhang, Q. Zhang, Q. Li, H. Bao, J. Zhou, S. Miao, N. Chen, J. Wang, B. Jiang, C. Tian and H. Fu, *Adv. Mater.*, 2020, **32**, 2003082; (f) F. Su, S. C. Mathew, G. Lipner, X. Fu, M. Antonietti, S. Blechert and X. Wang, *J. Am. Chem. Soc.*, 2010, **132**, 16299–16301; (g) X. Chen, J. Zhang, X. Fu, M. Antonietti and X. Wang, *J. Am. Chem. Soc.*, 2009, **131**, 11658–11659.

11 (a) I. Ghosh, J. Khamrai, A. Savateev, N. Shlapakov, M. Antonietti and B. König, *Science*, 2019, **365**, 360–366; (b) F. Goettmann, A. Fischer, M. Antonietti and A. Thomas, *Angew. Chem., Int. Ed.*, 2006, **45**, 4467–4471; (c) F. Goettmann, A. Fischer, M. Antonietti and A. Thomas, *Chem. Commun.*, 2006, 4530–4532; (d) F. Goettmann, A. Fischer, M. Antonietti and A. Thomas, *New J. Chem.*, 2007, **31**, 1455–1460; (e) G. Filippini, F. Longobardo, L. Forster, A. Criado, G. Di Carmine, L. Nasi, C. D'Agostino, M. Melchionna, P. Fornasiero and M. Prato, *Sci. Adv.*, 2020, **6**, eabc9923.

12 (a) Y. Wang, J. Yao, H. Li, D. Su and M. Antonietti, *J. Am. Chem. Soc.*, 2011, **133**, 2362–2365; (b) G. Vilé, D. Albani, M. Nachtegaal, Z. Chen, D. Dontsova, M. Antonietti, N. López and J. Pérez-Ramírez, *Angew. Chem., Int. Ed.*, 2015, **54**, 11265–11269.

13 (a) M. Baar and S. Blechert, *Chem. – Eur. J.*, 2015, **21**, 526–530; (b) F. Su, S. C. Mathew, L. Möhlmann, M. Antonietti, X. Wang and S. Blechert, *Angew. Chem., Int. Ed.*, 2011, **50**, 657–660; (c) X. Zhao, C. Deng, D. Meng, H. Ji, C. Chen, W. Song and J. Zhao, *ACS Catal.*, 2020, **10**, 15178–15185; (d) B. Pieber, M. Shalom, M. Antonietti, P. H. Seeberger and K. Gilmore, *Angew. Chem., Int. Ed.*, 2018, **57**, 9976–9979; (e) Y. Dai, C. Li, Y. Shen, T. Lim, J. Xu, Y. Li, H. Niemantsverdriet, F. Besenbacher, N. Lock and R. Su, *Nat. Commun.*, 2018, **9**, 60; (f) G. Song, W. Zhang, J. Song, Q. Li, Y. Feng, H. Liang, T. Kang, J. Dong, G. Li, J. Fan, X.-P. Zhang, Q. Gu, C. Wang and D. Xue, *Nat. Commun.*, 2025, **16**, 7045; (g) B. Dam, A. K. Sahoo and B. K. Patel, *Green Chem.*, 2022, **24**, 7122–7130.

14 (a) C. Wang, B. Hu, X. Guo and L. Lei, *Green Chem.*, 2024, **26**, 6470–6479; (b) A. J. Rieth, Y. Qin, B. C. M. Martindale and D. G. Nocera, *J. Am. Chem. Soc.*, 2021, **143**, 4646–4652; (c) A. Actis, M. Melchionna, G. Filippini, P. Fornasiero, M. Prato, M. Chiesa and E. Salvadori, *Angew. Chem., Int. Ed.*, 2023, **62**, e202313540; (d) J. Wang, S. Yin, Q. Zhang, F. Cao, Y. Xing, Q. Zhao, Y. Wang, W. Xu and W. Wu, *J. Catal.*, 2021, **404**, 89–95.

15 (a) T. Kooaira, K. Hayashi and T. Ohnishi, *Polym. J.*, 1973, **4**, 1–9; (b) T. Pirman, M. Ocepek and B. Likozar, *Ind. Eng. Chem. Res.*, 2021, **60**, 9347–9367.

16 S. Bishi, B. S. Lenka, P. Kreitmeier, O. Reiser and D. Sarkar, *Adv. Synth. Catal.*, 2024, **366**, 3397–3403.

17 Z. Liu, C. Zhou, T. Lei, X.-L. Nan, B. Chen, C.-H. Tung and L.-Z. Wu, *CCS Chem.*, 2020, **2**, 582–588.

18 J. Guo, Q. Xia, W. Y. Tang, Z. Li, X. Wu, L.-J. Liu, W.-P. To, H.-X. Shu, K.-H. Low, P. C. Y. Chow, T. W. B. Lo and J. He, *Nat. Catal.*, 2024, **7**, 307–320.

19 M. Golfmann, L. Glagow, A. Giakoumidakis, C. Golz and J. C. L. Walker, *Chem. – Eur. J.*, 2023, **29**, e202202373.

20 (a) C. Yang, R. Li, K. A. I. Zhang, W. Lin, K. Landfester and X. Wang, *Nat. Commun.*, 2020, **11**, 1239.

21 L. Guo, R. Chu, X. Hao, Y. Lei, H. Li, D. Ma, G. Wang, C.-H. Tung and Y. Wang, *Nat. Commun.*, 2024, **15**, 979.

22 Y. Hashimoto, G. Horiguchi, H. Kamiya and Y. Okada, *Eur. J. Org. Chem.*, 2022, e202201208.

23 (a) T. R. Blum, Z. D. Miller, D. M. Bates, I. A. Guzei and T. P. Yoon, *Science*, 2016, **354**, 1391–1395; (b) T. Lei, C. Zhou, M.-Y. Huang, L.-M. Zhao, B. Yang, C. Ye, H. Xiao, Q.-Y. Meng, V. Ramamurthy, C.-H. Tung and L.-Z. Wu, *Angew. Chem., Int. Ed.*, 2017, **56**, 15407–15410.

24 Y. Fu, Y. Xia, Y. Xu, X. Ye, S. Xie, Y. Wu, W. Zhao and F. Zhong, *ACS Sustainable Chem. Eng.*, 2023, **11**, 17752–17759.

25 F. Pellegrino, L. Pellutiè, F. Sordello, C. Minero, E. Ortel, V.-D. Hodoroaba and V. Maurino, *Appl. Catal., B*, 2017, **216**, 80–87.

26 Y. Liu, M. Zhang, C.-H. Tung and Y. Wang, *ACS Catal.*, 2016, **6**, 8389–8394.